



International Conference On Medical Imaging Understanding and Analysis 2016, MIUA 2016,  
6-8 July 2016, Loughborough, UK

## Hybrid Level-Sets for Vertebral Body Segmentation in Clinical Spine MRI

Georg Hille<sup>a,\*</sup>, Sylvia Glaßer<sup>a</sup>, Klaus Tönnies<sup>a</sup>

<sup>a</sup>Department of Simulation and Graphics, University of Magdeburg, Universitätsplatz 2, 39106 Magdeburg, Germany

### Abstract

In clinical routine, spine pathologies can be most often deduced from the vertebral body shape, position and orientation. Additionally, per-vertebra spatial information could be used in intervention planning and surgical navigation. Especially in vertebral metastasis treatment, MRI is invaluable, and therefore, segmentation methods are developed for spine MRI. Our approach starts with a simple user-assisted initialization. Then intensity and edge features are combined for a subsequent hybrid level-set segmentation. We evaluated our method on highly anisotropic clinical routine spine MRI datasets, containing 34 vertebrae, both healthy and pathological. We achieved a 3D Dice coefficient of 84.8 % and a mean surface-to-surface distance of  $1.29 \pm 0.42$  mm with regard to a manually created ground truth segmentation. The main advantages of our method are precise segmentation results on clinical routine images within reasonable processing time and with minimal user interaction.

© 2016 The Authors. Published by Elsevier B.V. This is an open access article under the CC BY-NC-ND license (<http://creativecommons.org/licenses/by-nc-nd/4.0/>).

Peer-review under responsibility of the Organizing Committee of MIUA 2016

**Keywords:** Clinical Spine MRI; Level-Sets; Segmentation; Vertebral Bodies; Vertebrae; Precise

### 1. Introduction

For various medical evaluations in neuroradiological diagnosis, treatment planning and surgical navigation, the segmentation of anatomical structures such as vertebral bodies or spinal cords, is challenging in clinical routine. Segmentation of vertebral bodies with their resulting shapes, positions and orientations depicts a major step towards a precise and reliable diagnosis. Moreover, segmented vertebrae could also enhance the intervention and radiotherapy planning and navigation. Most common approaches for 3D vertebral body segmentation are based on CT images<sup>1,2</sup> and are hardly transferable to MRI datasets. In routine spine MRI, strongly anisotropic spatial resolution often results in partial volume effects. Therefore, edges are hardly detectable (see Figure 1). Besides bias field artifacts in MRI cause non-homogenous intensities between central and marginal areas, various parameters affect the image quality and emphasis of different tissue types. These MRI characteristics hamper automatic segmentation approaches, while manual segmentation is time-consuming and hardly reproducible.

\* Corresponding author

E-mail address: [georg.hille@ovgu.de](mailto:georg.hille@ovgu.de)

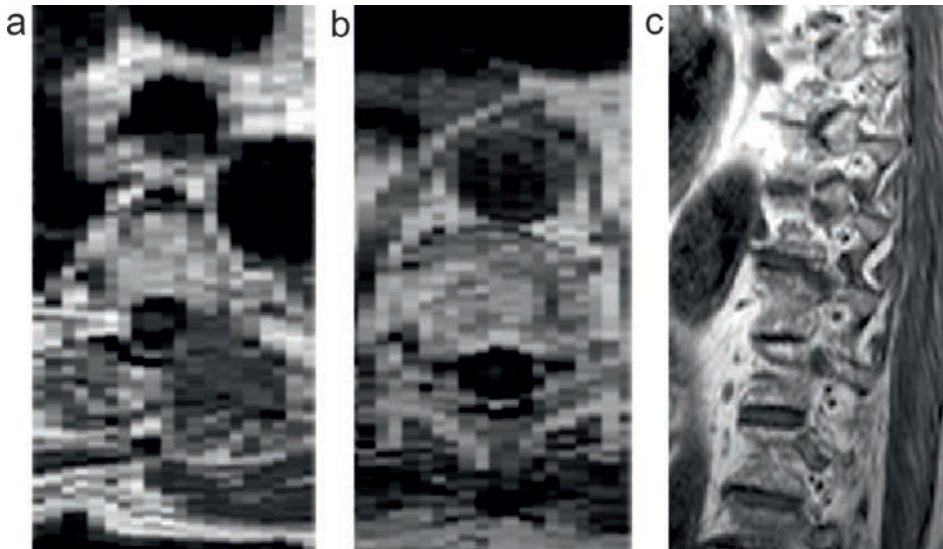


Fig. 1. A strongly anisotropic voxel size, like this particular MRI data set with 3.30 mm slice thickness and  $0.78 \times 0.78 \text{ mm}^2$  sagittal in-plane resolution, provokes partial volume effects, which hamper edge detection and automatic segmentation approaches. Depicted are axial slices of a thoracic (a) and a lumbar vertebra (b). The further away from mid-sagittal slices, the more complicated the distinction between bony vertebral and surrounding tissue gets (c).

Up to now, much research has been done on spinal segmentation, especially 2D methods like<sup>3,4</sup>. Their main disadvantage lies in processing only discrete slices. Thus, important information about vertebral body shape or orientation is omitted. A few 3D segmentation approaches were presented for MRI, which we will discuss below.

Hoad and Martel<sup>5</sup> presented a combination of a thresholded region-growing algorithm with morphological filtering and shape masking for segmenting vertebral bodies and posterior structures in isotropic ( $1 \times 1 \times 1 \text{ mm}^3$ ) steady state precession acquisition sequence images. Their method was designed for this particular case, rather than for anisotropic clinical routine spine MRI. In addition, another popular segmentation technique is based on deformable models, e.g., active contour models (ACM)<sup>6,7</sup> or active shape models (ASM)<sup>8</sup>. Davatzikos et al.<sup>9</sup> trained a deformable shape model to register image data with template images. They achieved an average overlap of  $81.5 \pm 3.6 \%$  on routine images of healthy volunteers with a spatial resolution of  $0.93 \times 0.93 \times 3 \text{ mm}^3$ . Štern et al.<sup>10</sup> also applied a model-based approach, while optimizing 29 shape parameters by maximization of the dissimilarity between inner and outer object intensities guided by image gradients. Evaluated on 75 vertebral bodies of nine subjects, their approach resulted in a radial Euclidean distance between segmented object surface and ground truth points of  $1.85 \pm 0.47 \text{ mm}$ . Neubert et al.<sup>11,12</sup> used active shape models to segment vertebral bodies and intervertebral discs alike. They tested their fully automatic approach on 14 healthy volunteers with 132 vertebrae, acquired with high resolution MRI ( $0.34 \times 0.34 \times 1$  to  $1.2 \text{ mm}^3$ ) They obtained a mean Dice similarity coefficient of 91 % and a mean Hausdorff distance of 4.08 mm. However, the average running time per vertebra of 35 min<sup>12</sup> must be considered. Hence, an entire data set required approximately 5 h computing time. Ayed et al.<sup>13</sup> pursued the idea of formulating the segmentation in MRI as a distribution-matching problem with a convex relaxation solution. For efficient computation, they split their problem into various sub-problems, where each one could be solved via convex relaxation and the augmented Lagrangian method. A mean Dice similarity coefficient of 85 % was achieved, but it was only determined on 2D mid-sagittal slices. Zukić et al.<sup>14</sup> combined edge and intensity-based features, i.e. Canny edges and thresholded gradient magnitudes to a multiple-feature-based model. The surface mesh of their model was enlarged by balloon forces and constrained by smoothness and the approximated vertebral body size. They achieved an average Dice similarity coefficient of 79.3 % with regard to a manual reference and a mean surface-to-surface distance of  $1.76 \pm 0.38 \text{ mm}$ , while evaluating on datasets containing both healthy and pathological vertebrae.

In this paper, we apply a 3D hybrid level-set approach based on the method by Zhang et al.<sup>15</sup> to segment vertebral bodies in MRI data from clinical routine with highly anisotropic spatial resolution. The evaluation set contains both

healthy and a few pathological vertebrae of the thoracic and the lumbar spine. For clinical applicability our method has to be reasonably fast and without inconvenient user input or previous learning. Therefore, we initialize our method with a simple three-point click to approximate the size and center of the desired vertebral bodies. If a higher degree of automation is required, existing vertebrae detection<sup>16</sup> or pre-registration<sup>17</sup> approaches could be used instead of manual initialization. Subsequently, intensity and edge features within a cylindrical region around each vertebral body are combined to provide a propagation field to steer the level-set algorithm. Our approach enables per-vertebra segmentation, because it is not dependent on prior segmentation results. It is efficient through short running times and a simple initialization and requires no learning or previous training.

## 2. Material and Methods

### 2.1. Image data

Sagittal T1-weighted turbo-spin-echo (TSE) images of thoracic and lumbar spine sections were acquired from 1.5 T and 3 T MR scanners. They contained both healthy and pathological vertebrae of six subjects, examined pre-interventionally for radiofrequency ablation (RFA) of vertebral metastasis. The clinical routine MRI scans had an in-plane resolutions between  $0.46 \times 0.46 \text{ mm}^2$  and  $0.78 \times 0.78 \text{ mm}^2$  and a slice thickness of 3.3 mm. The manual segmentation of the ground truth was performed by two independent trained field experts.

### 2.2. Methodology

Image segmentation using active contours is based on iteratively evolving an initial curve towards object boundaries, steered by a combination of internal forces and constrained by the curve geometry and external forces induced from the image. Usually, the segmentation is defined as a functional minimization problem targeting object boundaries. The usage of a hybrid level-set algorithm based on the approach presented by Zhang et al.<sup>15</sup> requires intensity and gradient features and an approximative geometry of the target object for steering and constraining the curve towards vertebral body boundaries.

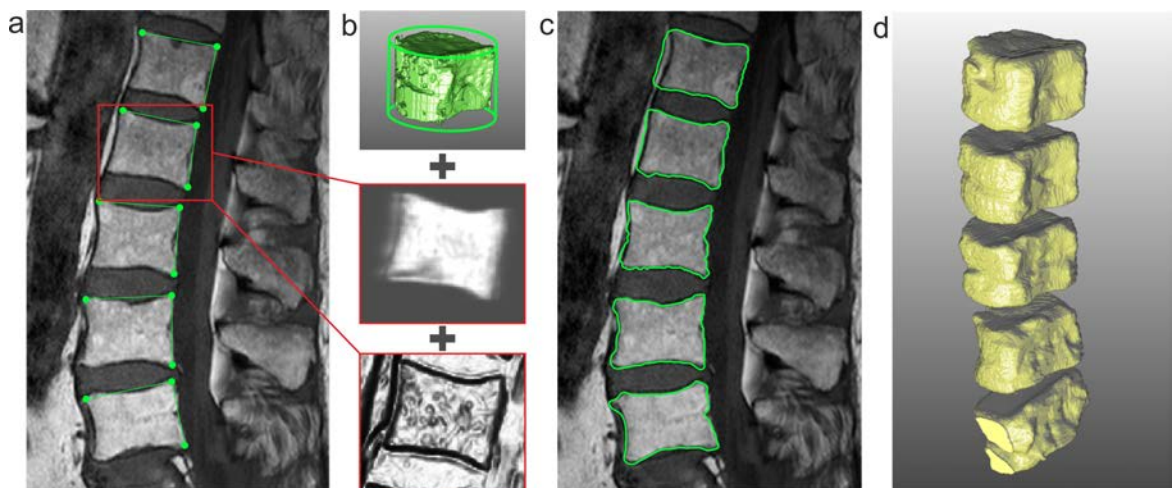


Fig. 2. Initialization of each vertebra with three-point clicks in the mid-sagittal cross-section enables the approximation of the vertebral body size and center (a). The hybrid level-set algorithm, combining a thresholded pre-segmentation within a cylindrical shape with intensity and gradient features (b), results in a 3D contour, which could be visualized as an overlay in each cross-section (c) or as a segmented 3D object (d).

The major steps of our approach are depicted in Figure 2. First, we used cubic interpolation to provide isotropic spatial resolution for each image data set. Subsequently, we initialized our method with a simple three-point click in the mid-sagittal cross-section to approximate the size and center of each vertebral body. Intensity-based features

were obtained from a cube with 5 mm edge length inside each vertebral body. Afterwards, a cylindrical bounding box was built around each vertebral body. Its radius equals 1.5 times the approximate vertebral body length and its height equals 1.2 times the approximate vertebral body height. Both measures were obtained during initialization. The cylinder was centered at the approximate vertebral body center and rotated around the lateral axis of the vertebra to fit orientation. Within the cylinder, a thresholded pre-segmentation based on the intensity information took place, followed by morphological filtering to estimate the vertebral body shape and to define the initial contour. The pre-segmentation was Gauss-filtered and combined with intensity statistics to yield the propagation field  $P$  in the regional term of the hybrid level-set formulation 1:

$$\mathcal{E}(\phi) = -\alpha \int_{\Omega} P \cdot H(\phi) d\Omega + \beta \int_{\Omega} g |\nabla H(\phi)| d\Omega. \quad (1)$$

The propagation field encourages the active contours to enclose regions of a specific per-vertebra gray-level range within the pre-segmentation.  $\mathcal{E}(\phi)$  is the functional to be minimized, whereby the Riemannian space induced from the image is searched for a minimum-length curve<sup>15</sup>. The image gradient field  $g$  defined the functional of the geodesic active contour term in the hybrid level-set formulation, whereby the contour should approach regions of high image gradients.  $H(\phi)$  represents the Heaviside function,  $\Omega$  the image domain and the weights  $\alpha$  and  $\beta$  were used to balance both terms. In our implementation, we weighted the region term empirically determined with 0.375 and the geodesic active contour term with 0.625. Thus, the boundary information achieves precise segmentation results, avoiding leakage problems due to the region term.

### 2.3. Evaluation

We tested our approach on six datasets, containing 34 vertebrae. A ground truth segmentation was manually created by two field experts. To examine the segmentation expertise, both manually segmented datasets were matched with each other. Due to comparability with related works, we evaluated the segmentation quality by using the Dice similarity coefficient both in 3D and in mid-sagittal slice, Hausdorff distance and mean surface-to-surface distance between the reference and our segmentation.

## 3. Results

First, the segmentation expertise of both field experts was checked, whereby a mean Dice coefficient with 90.3 % was the outcome of the expertise check performed by Zukić et al.<sup>14</sup>. Furthermore, all results are averaged referring to the manual segmentations of both field experts. The processing time per vertebra, depending on the spatial resolution or examined spine segment, never exceeded 60 s.

With an average Dice coefficient of all segmented vertebral bodies of 84.8 % our approach is significantly better than Zukić et al.<sup>14</sup> with 79.3 % or Davatzikos et al.<sup>9</sup> with 81.5 %, whereas the latter only tested their method on healthy subjects. Obviously, the segmentation quality decreases with pathologies like vertebral metastasis or severe deformations. Compared to Zukić et al.<sup>14</sup>, our approach exploited the advantage of a better adaption of individual vertebrae measures by our initialization method. By determining only mid-sagittal Dice coefficients we could match with the works of Ayed et al.<sup>13</sup>, Ghosh et al.<sup>18</sup> and Huang et al.<sup>4</sup>, while clearly outperforming the first two methods with a Dice coefficient of 93.5 % in comparison to their reported 85 % and 79 %, respectively. Huang et al.<sup>4</sup> achieved slightly higher segmentation precision with a mid-sagittal Dice coefficient of 96 %, though they tested their approach only on healthy subjects.

To compare our method with those of Štern et al.<sup>10</sup> or Kadoury et al.<sup>19</sup>, we furthermore determined the mean surface-to-surface distance, though direct comparison is not straightforward. With  $1.29 \pm 0.42$  mm we achieved better results than Štern et al.<sup>10</sup>, who report a mean error of  $1.85 \pm 0.47$  mm and Kadoury et al.<sup>19</sup> with  $2.1 \pm 0.8$  mm. Both works used isotropic or almost isotropic MRI datasets. Our method also outperformed the work of Zukić et al.<sup>14</sup>, who also dealt with highly anisotropic datasets and obtained a mean distance error of  $1.76 \pm 0.38$  mm.

Neubert et al.<sup>12</sup> presented the best overall segmentation quality with a 3D Dice coefficient of 90.8 % (vs. our 84.8 %), a mean Euclidean distance error of 0.67 mm (vs. our  $1.28 \pm 0.42$  mm) and an average Hausdorff distance of 4.07 mm (vs. our 6.55 mm) and consequently outperformed our method. However, their high quality comes at a cost of

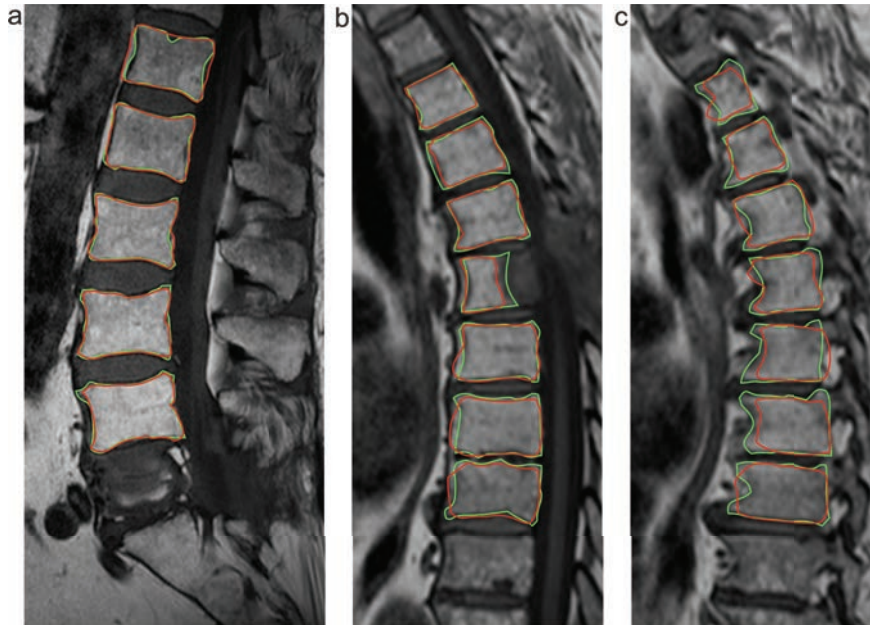


Fig. 3. Overlay of our resulting and the reference segmentation (images were cropped to save space). Green contours correspond to the reference segmentations and red contours illustrate the automatic segmentation results. Mid-sagittal cross-sections of two subjects (a and b) and a lateral cross-section of the second subject are shown (c). The mean 3D Dice coefficients of those datasets were 90.0 % and 83.7 %, respectively.

a considerably longer processing time per vertebral body of 35 min on recent hardware. Additionally, they tested their approach only on high-resolution MR images. While comparing distance errors, it is necessary to consider that higher mean distances may partially result from larger inter-slice spacing. A 10-fold processing time reduction decreases their Dice coefficient from 90.8 %<sup>12</sup> to 85 %<sup>11</sup>, which is similar to ours. Most discrepancies between the reference and our semi-automatic segmentation arise from lateral slices, caused by the impact of partial volume effects, which hardens the algorithmic detection of object boundaries (see Figure 3).

#### 4. Conclusion

We extended the hybrid level-set method presented by Zhang et al.<sup>15</sup> and applied it to vertebral body segmentation in MRI. Our approach is reasonably fast and robust on anisotropic and low resolution MRI data acquired in a clinical routine. The hybrid level-set combines regional intensity features and a boundary feature map related to image gradients. The semi-automatic initialization with approximate vertebral body center and size determination increases the robustness of segmentation with regard to the spine section, image resolution and deforming pathologies. Compared to related approaches in the literature, our method achieves similar or even better results. In future work, the segmentation should be combined with automatic initial vertebrae detection and can also be employed as a prerequisite for co-registration of multimodal images.

#### 5. Acknowledgements

This work was supported by the German Ministry of Education and Research under grant number '13GW0095A' within the Forschungscampus STIMULATE.

## References

1. Ma, J., Lu, L.. Hierarchical segmentation and identification of thoracic vertebra using learning-based edge detection and coarse-to-fine deformable model. *Computer Vision and Image Understanding* 2013;**117**(9):1072–1083.
2. Klinder, T., Ostermann, J., Ehm, M., Franz, A., Kneser, R., Lorenz, C.. Automated model-based vertebra detection, identification, and segmentation in CT images. *Medical Image Analysis* 2009;**13**(3):471–482.
3. Rak, M., Tönnies, K.D.. On computerized methods for spine analysis in MRI: a systematic review. *International Journal of Computer Assisted Radiology and Surgery* 2016;:1–21.
4. S.-H., H., Chu, Y.H., Lai, S.H., Novak, C.L.. Learning-based vertebra detection and iterative normalized-cut segmentation for spinal MRI. *IEEE Transactions on Medical Imaging* 2009;**28**(10):1595–1605.
5. Hoad, C.L., Martel, A.L.. Segmentation of MR images for computer-assisted surgery of the lumbar spine. *Physics in Medicine and Biology* 2002;**47**(19):3503.
6. Kass, M., Witkin, A., Terzopoulos, D.. Snakes: Active contour models. *International Journal of Computer Vision* 1988;**1**(4):321–331.
7. Caselles, V., Kimmel, R., Sapiro, G.. Geodesic active contours. *International Journal of Computer Vision* 1997;**22**(1):61–79.
8. Cootes, T.F., Taylor, C.J., Cooper, D.H., Graham, J.. Active shape models-their training and application. *Computer Vision and Image Understanding* 1995;**61**(1):38–59.
9. Davatzikos, C., Liu, D., Shen, D., Herskovits, E.H.. Spatial normalization of spine MR images for statistical correlation of lesions with clinical symptoms 1. *Radiology* 2002;**224**(3):919–926.
10. Štern, D., Likar, B., Pernuš, F., Vrtovec, T.. Parametric modelling and segmentation of vertebral bodies in 3d CT and MR spine images. *Physics in Medicine and Biology* 2011;**56**(23):7505.
11. Neubert, A., Fripp, J., Shen, K., Salvado, O., Schwarz, R., Lauer, L., et al. Automated 3d segmentation of vertebral bodies and intervertebral discs from MRI. In: *Proceedings of Digital Image Computing Techniques and Applications (DICTA) 2011*. 2011, p. 19–24.
12. Neubert, A., Fripp, J., Engstrom, C., Schwarz, R., Lauer, L., Salvado, O., et al. Automated detection, 3d segmentation and analysis of high resolution spine MR images using statistical shape models. *Physics in Medicine and Biology* 2012;**57**(24):8357.
13. Ayed, I.B., Punithakumar, K., Minhas, R., Joshi, R., Garvin, G.J.. Vertebral body segmentation in MRI via convex relaxation and distribution matching. In: *Proceedings of Medical Image Computing and Computer-Assisted Intervention (MICCAI) 2012*. 2012, p. 520–527.
14. Zukić, D., Vlasák, A., Egger, J., Hořínek, D., Nimsky, C., Kolb, A.. Robust detection and segmentation for diagnosis of vertebral diseases using routine MR images. *Computer Graphics Forum* 2014;**33**(6):190–204.
15. Zhang, Y., Matuszewski, B.J., Shark, L.K., Moore, C.J.. Medical image segmentation using new hybrid level-set method. In: *Proceedings of BioMedical Visualization (MEDIVIS) 2008*. 2008, p. 71–76.
16. Rak, M., Engel, K., Tönnies, K.D.. Closed-form hierarchical finite element models for part-based object detection. In: *Proceedings of the International Workshop on Vision, Modeling and Visualization (VMV) 2013*. 2013, p. 137–144.
17. Hille, G., Glaßer, S., Riabikin, O., Tönnies, K.D.. Regionenbasierte rigide Bildregistrierung von präoperativen MR- und intraoperativen Dyna-CT-Bildern zur Interventionsunterstützung bei Wirbelkörpermetastasen. In: *Proceedings of Deutschen Gesellschaft für Computer- und Roboterassistierte Chirurgie (CURAC) 2015*. 2015, p. 175–180.
18. Ghosh, S., Malgireddy, M.R., Chaudhary, V., Dhillon, G.. A supervised approach towards segmentation of clinical MRI for automatic lumbar diagnosis. In: *Computational Methods and Clinical Applications for Spine Imaging*; vol. 17. 2014, p. 185–195.
19. Kadoury, S., Labelle, H., Paragios, N.. Spine segmentation in medical images using manifold embeddings and higher-order MRFs. *IEEE Transactions on Medical Imaging* 2013;**32**(7):1227–1238.